Butyration of Lignosulfonate with Butyric Anhydride in the Presence of Choline Chloride

Lifen Li, Yingcheng Hu,* and Fangchao Cheng

A novel process was developed for the butyration of lignosulfonate (LS) with butyric anhydride in the presence of choline chloride at elevated temperatures. The degree of substitution (DS) was qualitatively and quantitatively determined by Fourier transform infrared spectroscopy using the baseline method. It was found that the DS of butyrated LS products increased from 0 to the range of 0.41 to 2.14 with the addition of choline chloride, indicating that butyric anhydride-choline chloride is a novel and highly effective solvent for the butyration of LS. The DS of butyrated LS was dependent on choline chloride dosage, reaction temperature, reaction time, and the mass ratio of butyric anhydride to LS. Characterization results by proton nuclear magnetic resonance spectroscopy further demonstrated the occurrence of the butyration reaction. The results of thermogravimetric analysis showed that the thermal stability of the butyrated LS decreased with increasing degree of substitution.

Keywords: Lignosulfonate; Butyration; Choline chloride; Spectroscopy; Thermal stability

*Contact information: Key Laboratory of Bio-based Material Science and Technology of Ministry of Education of China, College of Material Science and Engineering, Northeast Forestry University, Harbin, China; *Corresponding author: yingchenghu@163.com*

INTRODUCTION

Lignin is one of the most abundant natural polymers on earth, along with cellulose and chitin (Wang *et al.* 2013). Annually, over 50 million tons of lignin are produced as a byproduct of the pulp and paper industry, but only a small amount of lignin is used in simple applications and energy production (Zakzeski *et al.* 2010). Development of new composites based on lignin is one strategy to enhance the use of this abundantly available byproduct. Such an approach has potential to lower the costs of blended composites and reduce pollution related to petroleum-based polymer materials. The most straightforward application is the use of lignin as a copolymer or polymer additive in thermoplastics, thermosetting matrices, and rubber polymers (Thielemans and Wool 2005). However, inherent differences in the physical and chemical properties of lignin and polymer matrices affect their compatibility (Sailaja and Deepthi 2010; Maldhure *et al.* 2011). For instance, heterogeneous nucleation of lignin in a polypropylene (PP) and poly(3-hydroxybutyrate) matrix was observed in previous work (Canetti *et al.* 2004; Grunden and Sung 2004), which could decrease the quality of the blended composites.

Recently, significant effort has been made to enhance the use of lignin in bio-based polymers *via* chemical modifications such as esterification, phenolation, etherification, urethanization, and others (Laurichesse and Avérous 2014). Esterification could improve the physiochemical properties of lignin and enhance the interfacial bonding between lignin and polymer materials by substituting hydroxyl groups (-OH)

with acyl groups (-COR), predominately through reactions with acid chlorides or anhydrides (Bridson *et al.* 2013). The solubility of the resulting lignin esters in non-polar solvents would be improved as hydrogen bonding sites are removed.

Previous investigations have shown that lignin butyrate, lignin maleate, and lignin phthalate can be used as additives in commercial polymers (Thielemans and Wool 2004; Maldhure *et al.* 2012; Lisperguer *et al.* 2013; Gordobil *et al.* 2014). Among these, lignin butyrate has been shown to be completely soluble in styrene, one of the most commonly used reactive diluents in unsaturated thermosetting polymers (Thielemans and Wool 2005). It has also been demonstrated that lignin butyrate could be used as a compatibilizing agent for natural fiber-reinforced thermoset composites, and the flexural strength of the blended composites containing 5wt% butyrated lignin exceeded that of the resin containing no butyrated lignin (Thielemans and Wool 2004). Further, butyrated lignin is more stable and resistant against UV light, which could inhibit photo-discoloration of lignin-containing materials (Chang *et al.* 2006).

The conventional lignin butyration reaction proceeds using butyric anhydride as the acylation agent in the presence of 1-methyl imidazole as a catalyst. However, this catalyst is harmful to humans and the environment. Lignosulfonate (LS), a byproduct of the sulfite process of the pulp and paper industries, is a valuable raw material because it is an abundant, low-cost, biodegradable resource. Unfortunately, the polarity of LS is large due to the sulfonate groups of the aliphatic side chains. Therefore, it is difficult to dissolve or esterify of LS in non-aqueous solvent, and few studies have addressed acylation of LS or other modifications of LS for incorporation into polymer matrices (Alonso *et al.* 2001; Lin *et al.* 2011; Bahl and Jana 2014).

The specific objective of the present work was to develop a simple and fast butyration pathway for LS using butyric anhydride in the presence of choline chloride without the use of a toxic catalyst (Glasser and Jain 1993). Typically, butyric anhydride reacts with the hydroxyl groups of LS to form LS esters and butyric acid byproducts, as shown in Fig. 1. The effects of certain reaction parameters, including the ratio of butyric anhydride-to-choline chloride, the reaction temperature, the reaction time, and the ratio of butyric anhydride-to-LS on the degree of substitution (DS) of the butyrated LS were studied. Fourier transform infrared (FTIR) spectroscopy and proton nuclear magnetic resonance (^{1}H NMR) spectroscopy were performed to investigate the reaction. A second objective was to characterize the thermal stability properties of the butyrated LS. Thermogravimetric (TG) analysis of LS samples with different DS was performed, and the kinetics of the thermal reaction was studied.

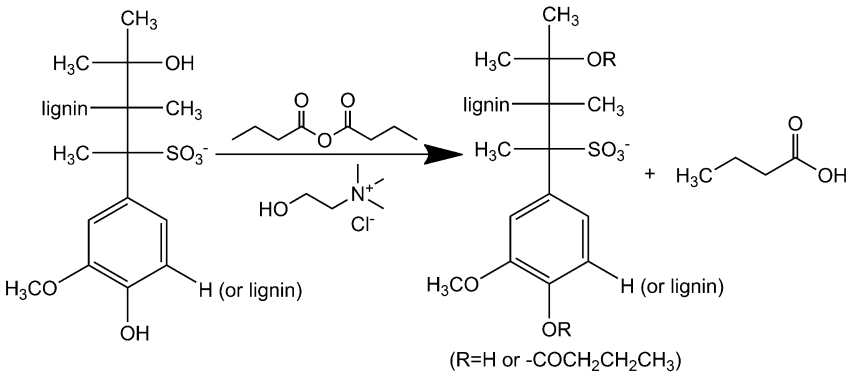

Fig. 1. Reaction of LS in butyric anhydride-choline chloride solvent

EXPERIMENTAL

Materials

Lignosulfonate (alkali lignin, low sulfonate content) and choline chloride (reagent grade) were purchased from Sigma-Aldrich (Shanghai, China), and were dried at 60 °C under vacuum for 12 h before use. Butyric anhydride (reagent grade) was supplied by the Aladdin Industrial Corporation, Shanghai.

Methods

Butyration of LS

The modification of LS was conducted in closed glass vials equipped with magnetic agitators in an oil bath, the temperature of the butyration process was controlled by the oil bath, and the recording thermometers was accurate to within ±1°C. The typical procedure for the butyration of LS was as follows: According to different mass ratio, a certain amount of LS and choline chloride were simultaneously added into 8 g of preheated butyric anhydride and then the resulting mixture was stirred for several minutes. Once the designated reaction time had elapsed, the reaction mixture was cooled to ambient temperature in a water bath before the contents were slowly poured into ethanol. The precipitated LS samples were collected *via* vacuum filtration and thoroughly washed with ethanol. Finally, the samples were dried at 60 °C for 18 h in an oven.

Analyses

The chemical structure of the LS derivatives was evaluated by FTIR (Nicolet 6700, Thermo Fisher Scientific, USA) with a Diamond Attenuated Total Reflectance (ATR) Smart Accessory. The acquisition conditions were a spectral width of 4000 to 650 cm^{-1} and a resolution of 4 cm^{-1}.

Proton nuclear magnetic resonance (^{1}H-NMR) spectra were obtained at room temperature on the Bruker-500 (Avance DRX-500, Bruker, Switzerland) NMR spectrometer. The ^{1}H spectra of butyric anhydride-choline chloride solvent were recorded in D_2O. The LS samples, weighing about 10 mg, were added into 0.5 mL of d_6-DMSO and left for several days to ensure complete dissolution. The spectral width was 5000 Hz, and the number of complex points collected was 1024 with a recycle delay of 1.5 s.

The thermal stability of unmodified LS and butyrated LS with different DS was analyzed using thermogravimetric analysis (Perkin Elmer, STA 6000, USA). Roughly 10-mg samples were heated from 40 to 800 °C at a heating rate of 10 °C/min under nitrogen flow. The residues at 800 °C were defined as ashes. The kinetic parameters of the thermal degradation of unmodified and butyrated LS products were determined using the Coats-Redfern method of thermogravimetry data processing.

RESULTS AND DISCUSSION

FTIR Spectra

Figure 2 shows the FTIR spectra of unmodified LS (spectrum a), LS butyrated at 120 °C for 20 min with pure butyric anhydride (spectrum b), and LS butyrated with butyric anhydride in the presence of 10 wt.% choline chloride (spectrum c). In spectrum 2a, the typical lignin peaks were visible, and the main assignments of FTIR bands are summarized in Table 1.

Table 1. Main Band Assignments in LS FTIR Spectrum (Faix 1991)

Band position (cm^{-1})	Assignment
3362	O-H stretching
2932, 2838	C-H stretching in CH_2 and CH_3 groups
1584, 1502	Aromatic skeletal vibrations
1451	Asymmetric C-H deformation of CH_2 and CH_3 groups
1417	Aromatic skeleton vibrations combined with C-H in-plane deformation
1371	Aliphatic C-H stretching in CH_3 groups
1259	C-O stretching of guaiacyl units
1129	Aromatic C-H in-plane deformation
1079	C-O deformation in secondary alcohols and aliphatic ethers
1038	C-H(O) and C-O(C) stretching of first order aliphatic OH and ether groups
850	Aromatic C-H out-of-plane bending of guaiacyl units

Compared to spectra 2a and 2b, the differences in spectrum 2c for LS butyrated in butyric anhydride-choline chloride solvent indicate that the butyration reaction occurred. Marked changes in the bands at 3386, 2963, 2935, 2874, 1732, 1457, and 1134 cm^{-1} were observed. The broad peak centered at 3386 cm^{-1} representing O-H stretching vibration, and the intensity of this band decreased in spectrum 2c; in addition, the peak position showed a blue shift, which is likely because the hydrogen bonds between the hydroxyl groups of the LS molecule were destroyed when O-H groups were substituted to form butyryl groups (Watanabe *et al.* 2006). The increased intensity of C-H stretching peaks at 2963, 2935, 2874, and 1457 cm^{-1} indicate that new C-H bonds were introduced into the LS.

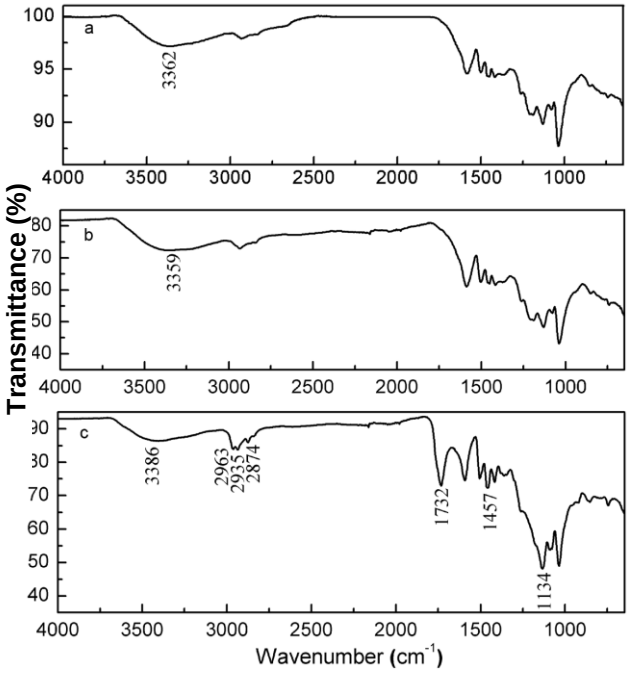

Fig. 2. FTIR spectra of (a) unmodified LS, (b) LS butyrated at 120 °C for 20 min with pure butyric anhydride, and (c) LS butyrated with butyric anhydride in the presence of 10 wt.% choline chloride

The appearance of carbonyl bonds (C=O), as indicated by the peak at 1732 cm^{-1} and the enhanced C-O absorption band at 1134 cm^{-1}, confirm the formation of ester bonds following butyration (Chang *et al.* 2006). These noticeable changes in the absorption bands indicate that butyryl groups were grafted onto the LS, and that the butyration reaction of LS occurred in the butyric anhydride-choline chloride solvent under the given reaction conditions. As expected, the absence of an absorption region between 1840 and 1760 cm^{-1} in spectra 2b and 2c confirm that the products were free of unreacted butyric anhydride (Chen *et al.* 2012). The lack of a peak representing a carboxylic group at 1700 cm^{-1} in the spectra of the butyrated products indicates that the LS esters did not contain butyric acid byproducts.

Proposed Mechanism

As shown in Fig. 2, butyration of LS could not occur with pure butyric anhydride at 120 °C, even after 20 min. However, addition of choline chloride obviously improved the efficiency of LS butyration. Choline-based ionic liquids (succinic anhydride and glutaric anhydride) form when choline chloride and anhydride are mixed under heated conditions (Lopes *et al.* 2013). In this work, choline chloride could also react with butyric anhydride at high temperatures, resulting in the formation of a butyrylcholine chloride ionic liquid.

Recently, ionic liquids containing chloride anions have been shown to be good solvents for dissolving lignin via hydrogen bond interactions (Pu *et al.* 2007). Choline chloride-urea deep eutectic ionic liquid was effective for the N-alkylation of various aromatic primary amines, possibly due to the formation of hydrogen bonds between the ionic liquid and the aromatic amino group, which could activate the amino group and make it more reactive (Singh *et al.* 2011).

In addition, choline chloride-urea deep eutectic ionic liquid has also been demonstrated to be a versatile catalyst to facilitate the synthesis of β-substituted ketonic derivatives. A tentative mechanism involving the activation of unsaturated carbonyl compounds through hydrogen bonding with ionic liquids was proposed (Yadav and Shankarling 2014).

Consequently, a plausible mechanism for the butyration of LS in butyric anhydride-choline chloride solvent is proposed, as shown in Fig. 3. On one hand, the hydrogen bonds form between the butyrylcholine chloride ionic liquid and LS accelerate the dissolution of LS by breaking its intermolecular and intramolecular hydrogen bonds. On the other hand, the hydrogen bonding interactions between ionic liquid and LS could also increase the nucleophilicity of the hydroxyl groups of LS, resulting in the faster nucleophilic attack of butyric anhydride.

To validate the proposed mechanism, ^1H NMR spectra of butyric anhydride-choline chloride solvent obtained by stirring at 120 °C for 20 min in D_2O were recorded, and results are shown in Fig. 4. The peaks were assigned to butyrylcholine according to a previous work (Wyman and Macartney 2010), indicating that the mechanism proposed is reasonable. However, there were some differences in the spectra obtained from the solvent of the present study, and the additional peaks indicate the presence of butyric anhydride and butyric acid synthesized by hydrolysis of butyric anhydride with D_2O, as described in Fig. 4.

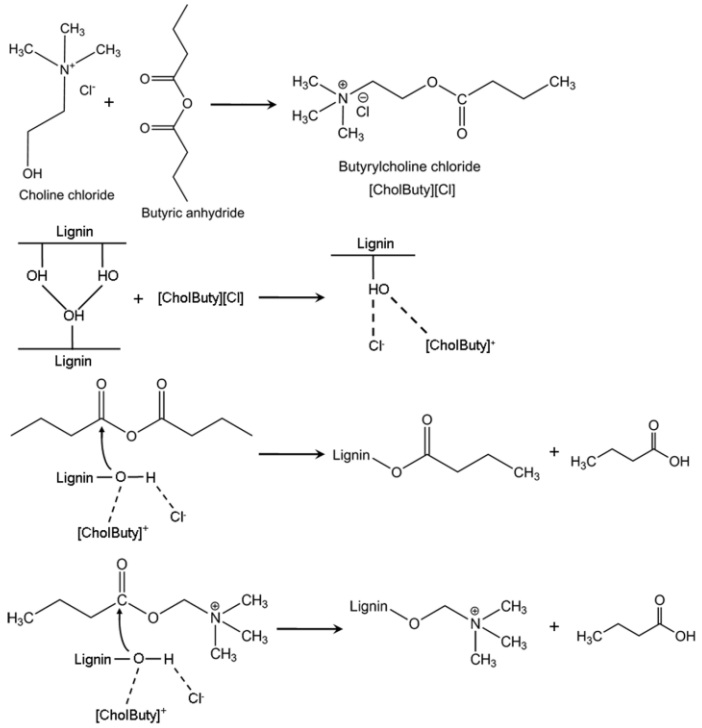

Fig. 3. Proposed mechanism for the butyration of LS in butyric anhydride-choline chloride solvent

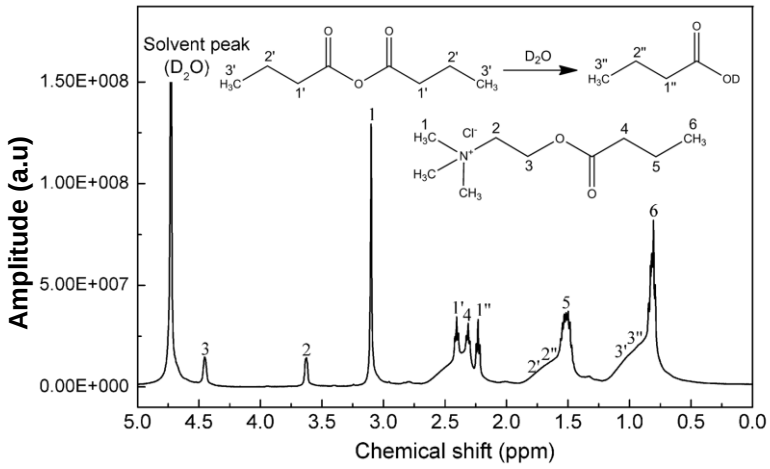

Fig. 4. Proton NMR spectra of butyric anhydride reacted in the presence of 10 wt.% choline chloride stirred at 120 °C for 20 min in D_2O

Degree of Substitution

Fourier transform infrared spectroscopy is appropriate for analyzing the chemical transformation of polymers by determining the intensity of specific bonds and functional groups within them (Tjeerdsma and Militz 2005). Thus, the DS was qualitatively and quantitatively analyzed with infrared spectra according to the relative peak intensities at 1732 cm^{-1} (acetyl C=O stretching band) and 1502 cm^{-1} (C=C stretching of aromatic skeleton) according to the methodology of previous studies (Fox and McDonald 2010; Cachet *et al.* 2014): $DS=A_{\sim 1732}/A_{\sim 1502}$. Here, 1502 cm^{-1} was used as an internal standard peak, as it was the same in all samples. The calculation results are listed in Table 2. As can be seen, the maximum DS of 2.14 was obtained using 15 wt.% choline chloride at

120 °C for 10 min. The synthesis of butyrated milled wood lignin having a DS of 1.68 ($A_{\sim1740}/A_{\sim1510}$) at 125 °C for 3 h has been reported in a previous study (Chang *et al.* 2006), whereas industrial lignin butyrate with a DS of 1.83 ($A_{\sim1740}/A_{\sim1500}$) was obtained at 65 °C for 24 h with 1-methylimidazole as a catalyst (Fox and McDonald 2010). Therefore, butyration of LS in the presence of choline chloride is an effective and time-saving method for the modification of LS.

Table 2. Degree of Substitution of Butyrated LS[a]

Sample Number	Choline chloride/Butyric anhydride (%)[b]	Temperature (°C)	Time (min)	Butyric anhydride/ LS (%)[b]	DS
1	0	120	20	4	0
2	5	120	10	4	1.14
3	10	120	10	4	1.83
4	15	120	10	4	2.14
5	20	120	10	4	1.84
6	10	90	10	4	0.41
7	10	100	10	4	0.92
8	10	110	10	4	1.71
9	10	120	5	4	0.45
10	10	120	15	4	1.68
11	10	120	20	4	1.32
12	10	120	10	3	1.74
13	10	120	10	2	1.66

[a] Estimated by FTIR analysis with according to relative intensities ($A_{\sim1732}/A_{\sim1502}$)
[b] Mass ratio

The linear relationship between $A_{\sim1457}/A_{\sim1502}$ and DS is shown in Fig. 5, where the peak at 1457 cm^{-1} corresponds to asymmetric C-H deformation vibration in the LS molecule and the butyric anhydride grafted onto the LS. It is noteworthy that the intensity of the absorption band of the LS molecule at 1457 cm^{-1} did not change following butyrylation (Gilarranz *et al.* 2001). Thus, the absorption intensity at 1457 cm^{-1} is associated with the grafting yield of the butyric anhydride. As can be seen in Fig. 5, a strongly positive correlation coefficient of 0.93 was obtained. Therefore, even if no precise value of DS was determined by FTIR, the ratio of $A_{\sim1732}/A_{\sim1502}$ can give an indication as to the degree of substitution of hydroxyl groups with butyryl groups in the butyrated LS with reasonable accuracy (Cachet *et al.* 2014). In an effort to optimize the reaction, a variety of variables were investigated, including the choline chloride dosage, reaction temperature, reaction duration, and the mass ratio of butyric anhydride-to-LS.

Effect of choline chloride dosage on the butyration of LS in butyric anhydride-choline chloride solvent

The effect of choline chloride dosage on the DS of LS esters was investigated according to the peak intensity of the butyrated LS samples, and the corresponding DS is illustrated in Table 2. Increasing the choline chloride dosage from 0 (sample 1) to 5 wt.% (sample 2), 10 wt.% (sample 3), and 15 wt.% (sample 4) improved the DS of the butyrated samples from 0 to 1.14, 1.83, and 2.14, respectively. The addition of choline chloride substantially improved the efficiency of the butyration reaction of LS compared to that of the control sample (1).

Further increase of choline chloride dosage from 15 to 20 wt.% (sample 5) resulted in a decrease in the DS of LS samples, from 2.14 to 1.84. This reduction can be explained in part by the decrease in the concentration of the esterifying agent with increasing choline chloride content.

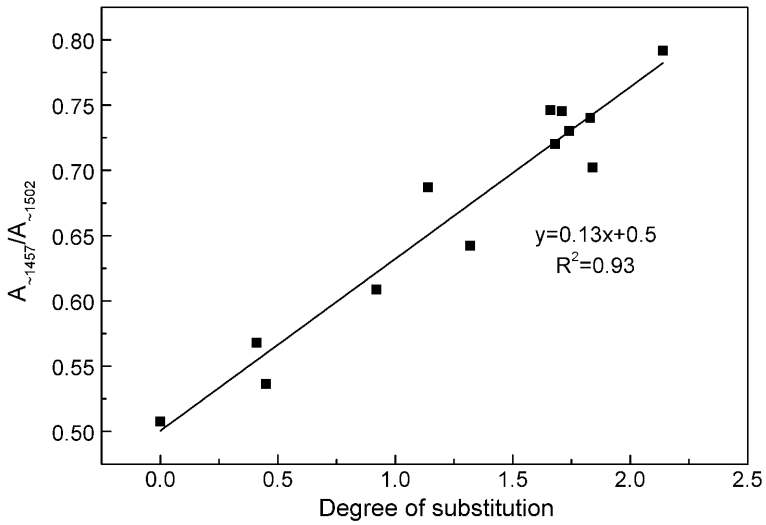

Fig. 5. Ratio of the peak areas at 1457 and 1502 cm^{-1} *versus* the DS of butyrated LS

Effect of reaction temperature on the butyration of LS in butyric anhydride-choline chloride solvent

Figure 6 shows the effect of reaction temperature on the absorption intensity in the FTIR spectra within the region between 1800 and 1100 cm^{-1}. The area of the peak at 1732 cm^{-1} increased with the heightened reaction temperature, indicating a positive influence of temperature on the butyration reaction. The reason for the high efficiency of butyration at higher temperatures was, presumably, the favorable effect of temperature on the mobility of the molecules involved in the reaction and the solubility of the LS in the ionic liquid, resulting in a greater molecular collision rate and more accessible O-H groups within the LS (Chadlia and Farouk 2011).

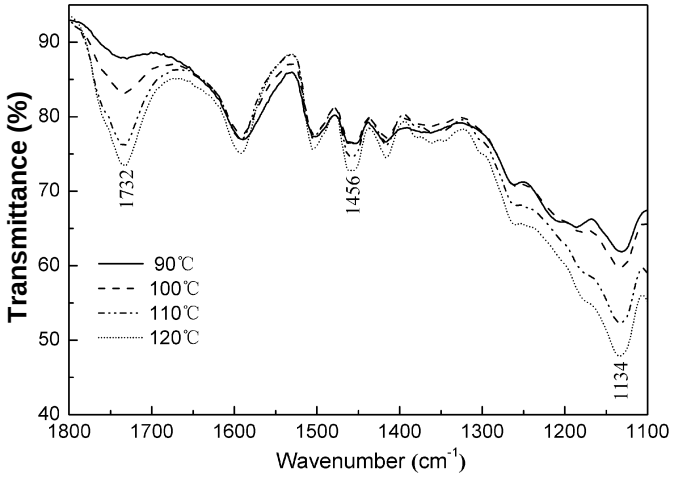

Fig. 6. FTIR spectra of butyrated LS prepared at different reaction temperatures for 10 min

Effect of reaction duration on the butyration of LS in butyric anhydride-choline chloride solvent

Increasing the reaction time from 5 min (sample 9) to 10 min (sample 3) resulted in an improvement in the DS of butyrated samples from 0.45 to 1.83 (Table 2). The enhancement of DS by prolonging the reaction was likely for two reasons. On one hand, more LS dissolved in the butyric anhydride-choline chloride solvent when the reaction duration was greater. Alternatively, increased reaction time corresponded to more molecular collisions between LS and the butyration reagent, thus causing the reaction to proceed more completely. However, further extension of the reaction time from 10 to 15 min (sample 10) and 20 min (sample 11) decreased the DS from 1.83 to 1.68 and 1.32, respectively, probably due to degradation or hydrolysis of LS esters during long reaction times (Chadlia and Farouk 2011). Therefore, 10 min was considered the optimal reaction time.

Effect of mass ratio of butyric anhydride to LS on the butyration of LS in butyric anhydride-choline chloride solvent

Maintaining the weight ratio of choline chloride to butyric anhydride at 10%, the reaction temperature at 120 °C, and the reaction time at 10 min, and decreasing the mass ratio of butyric anhydride-to-LS from 4:1 to 2:1 resulted in a decrease in the DS of the LS derivatives from 1.83 to 1.66 (Table 2). This decrease in the reaction efficiency happened because the relative content of dissolved LS was lower and the availability of butyric anhydride molecules in the proximity of the LS molecules was lesser at lower concentrations of the esterifying agent (Xiao *et al.* 2001).

NMR Spectroscopy

Another method used to determine the structure of polymers is NMR spectroscopy (Ye *et al.* 2013). The ^{1}H NMR spectra of unmodified LS (Fig. 7a) and LS butyrated in butyric anhydride-choline chloride solvent at 120 °C for 20 min (Fig. 7b, sample 11) are shown in Fig. 7. Clear differences can be observed between the spectra in Fig. 7b and Fig. 7a. Peak assignments were made on the basis of previous research (Thielemans and Wool 2005; Ye *et al.* 2013). The ^{1}H NMR spectra indicate protons in the aromatic ring at 7.7 to 6.1 ppm and protons in methoxyl groups (OCH_3) at 4.0 to 3.5 ppm. Signals at 3.5 to 3.1 ppm were assigned to the protons of the water in the solvent and the sharp signal at 2.5 ppm originated from the solvent itself (DMSO-d_6).

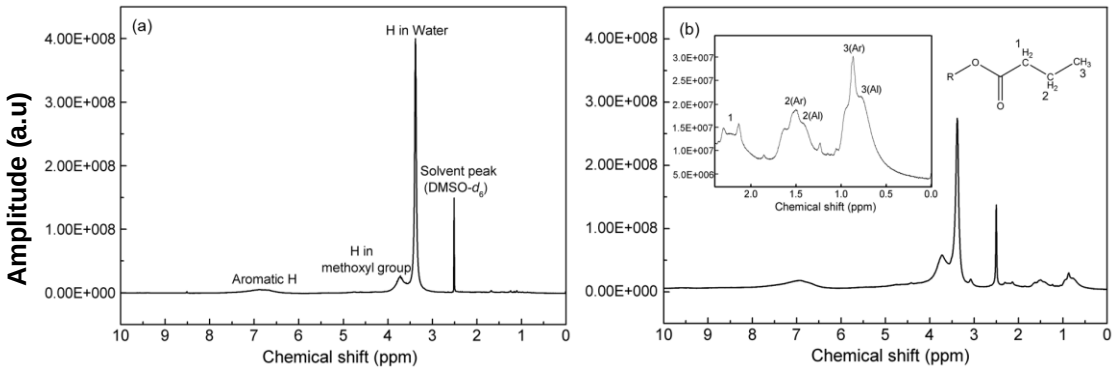

Fig. 7. (a) Proton NMR spectra of original LS and (b) LS butyrated with butyric anhydride in the presence of 10 wt.% choline chloride at 120 °C for 20 min (sample 11)

Compared with Fig. 7a, Fig. 7b has signals at 2.3 to 1.9 ppm, 1.7 to 1.2 ppm, and 1.0 to 0 ppm, corresponding to the protons in the CH_2 and CH_3 groups of LS butyrate. This phenomenon further demonstrates the occurrence of the butyration reaction in the butyric anhydride-choline chloride solvent and agrees with the results of FTIR analysis. It also implies that butyration of LS occurred at both phenolic and aliphatic hydroxyl groups.

Thermal Stability

To expand the potential applications of lignin and lignin derivatives, it is imperative that issues related to their thermal stability are addressed (Lin *et al.* 2008). Thermogravimetry is one of the techniques most widely used to monitor the change of mass of polymers throughout the thermal degradation process. Thermogravimetry measures the amount of weight change of substances as a function of temperature, while the first derivative thermogravimetric (DTG) curves show the corresponding rate of weight loss. The TG and DTG curves can both be used to compare the thermal stability characteristics of different materials.

The effect of butyration on the thermal properties of LS was examined using TG analysis in the temperature range of 40 to 800 °C.

The TG and DTG curves of the butyrated LS with different DS (LS_0, $LS_{0.45}$, $LS_{1.14}$, $LS_{1.32}$, and $LS_{1.68}$, representing LS esters with DS of 0, 0.45, 1.14, 1.32, and 1.68, respectively) are presented in Fig. 8.

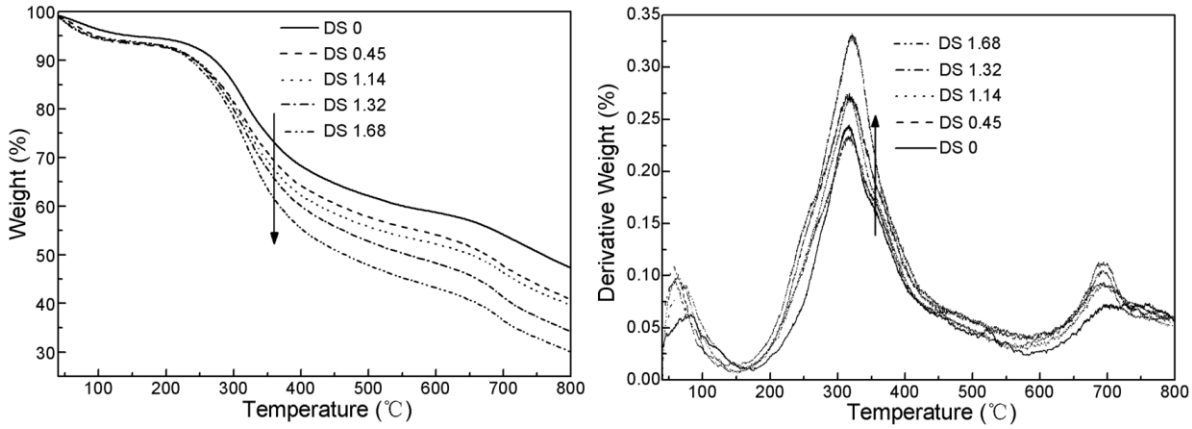

Fig. 8. Thermograms of butyrated LS with different DS

Three stages of LS degradation can be distinguished on the DTG curves of both the original and derivative LS. The DTG curves indicate an initial degradation stage at 40 to 150 °C, mainly due to the evaporation of absorbed water. Subsequently, a rapid decline in weight occurred, and the weight loss in this second stage was attributed to the fragmentation of the inter-unit linkages of LS and the evaporation of monomeric phenol (Tejado *et al.* 2007). The maximum weight loss rate in this stage was 0.22 %/°C at 314 °C for LS_0, 0.23 %/°C at 319 °C for $LS_{0.45}$, 0.27 %/°C at 320 °C for $LS_{1.14}$, 0.27 %/°C at 320 °C for $LS_{1.32}$, and 0.33 %/°C at 326 °C for $LS_{1.68}$, as obtained from the DTG curves. In the last stage, the rate of weight loss was lower, possibly due to further decomposition of LS samples. The ash contents at 800 °C also provided information as to the thermal stability of the LS. The ash contents were 47.35% for LS_0, 40.87% for $LS_{0.45}$, 39.70% for $LS_{1.14}$, 34.21% for $LS_{1.32}$, and 30.03% for $LS_{1.68}$, respectively.

According to the results of the TG and DTG curves, the thermal stability of unmodified LS was higher than that of the LS esters, indicating the negative effect of the butyration reaction on thermal stability. The changes in the thermodynamic stability of butyrated LS were probably due to the degradation, hydrolysis, and repolymerization of macromolecular LS under acidic conditions in the presence of butyric acid. Similar observations have has also been reported during the esterification of commercial alkali lignin in formamide, pyridine, and acetic acid anhydride reaction systems (Gordobil *et al.* 2014).

Thermogravimetric Kinetics

As kinetic analysis could effectively assist in understanding degradation mechanisms and predicting the thermal stability of polymers (Flynn 1989), there have been many studies regarding the kinetic analysis of lignin pyrolysis in recent years (Jiang *et al.* 2010). However, few studies about the pyrolysis kinetics of pure LS and esterified LS have been reported. The kinetic parameters of the thermal reaction of butyrated LS with different DS at a constant heating rate of 10 °C/min were calculated.

The pyrolysis kinetics of unmodified LS and butyrated LS samples were investigated according to the Coats-Redfern method (Coats and Redfern 1964), and the formulas determined are shown in Eqs. (1) and (2). The fundamental kinetic model used obeys the famous Arrhenius equation (Sait *et al.* 2012) and the rate of reaction is given by Eq. (3):

$$\ln[\frac{1-(1-\alpha)^{1-n}}{T^2(1-n)}] = \ln[\frac{AR}{\beta E}(1-\frac{2RT}{E})] - \frac{E}{RT} \quad (\text{for } n\neq 1) \tag{1}$$

$$\ln[\frac{-\ln(1-\alpha)}{T^2}] = \ln[\frac{AR}{\beta E}(1-\frac{2RT}{E})] - \frac{E}{RT} \quad (\text{for } n=1) \tag{2}$$

$$\frac{d\alpha}{dT} = \left(\frac{A}{\beta}\right)\exp\left(-\frac{E}{RT}\right)(1-\alpha)^n \tag{3}$$

where α is the fraction of solid material that has decomposed at time t as defined in Eq. (4), n is the order of the reaction, T is the absolute temperature (K), A is the frequency factor (min^{-1}), R is the gas constant (equal to 8.314 J/(mol·K)), β is the heating rate (°C/min), and E is the activation energy (KJ/mol).

$$\alpha = (W_0 - W_t)/(W_0 - W\infty) \tag{4}$$

Here, W_0, W_t, and W_∞ refer to the initial, instantaneous, and final masses, respectively.

To eliminate the influence of the water present in the LS, 150 °C was designated the initial temperature, and the ending temperature was set to 800 °C. The fast pyrolysis stage with weight loss rate higher than 0.1%/°C was observed in the temperature ranges of 261.09 to 393.29 °C for LS_0, 244.74 to 396.33 °C for $LS_{0.45}$, 243.77 to 398.53 °C for $LS_{1.14}$, 236.13 to 404.10 °C for $LS_{1.32}$, and 230.54 to 411.48 °C for $LS_{1.68}$. Figure 9 shows the linear regression curves of the LS samples in the fast pyrolysis stage, each of which had a favorable correlation coefficient (greater than 0.9978), demonstrating that the order of the reaction selected was appropriate.

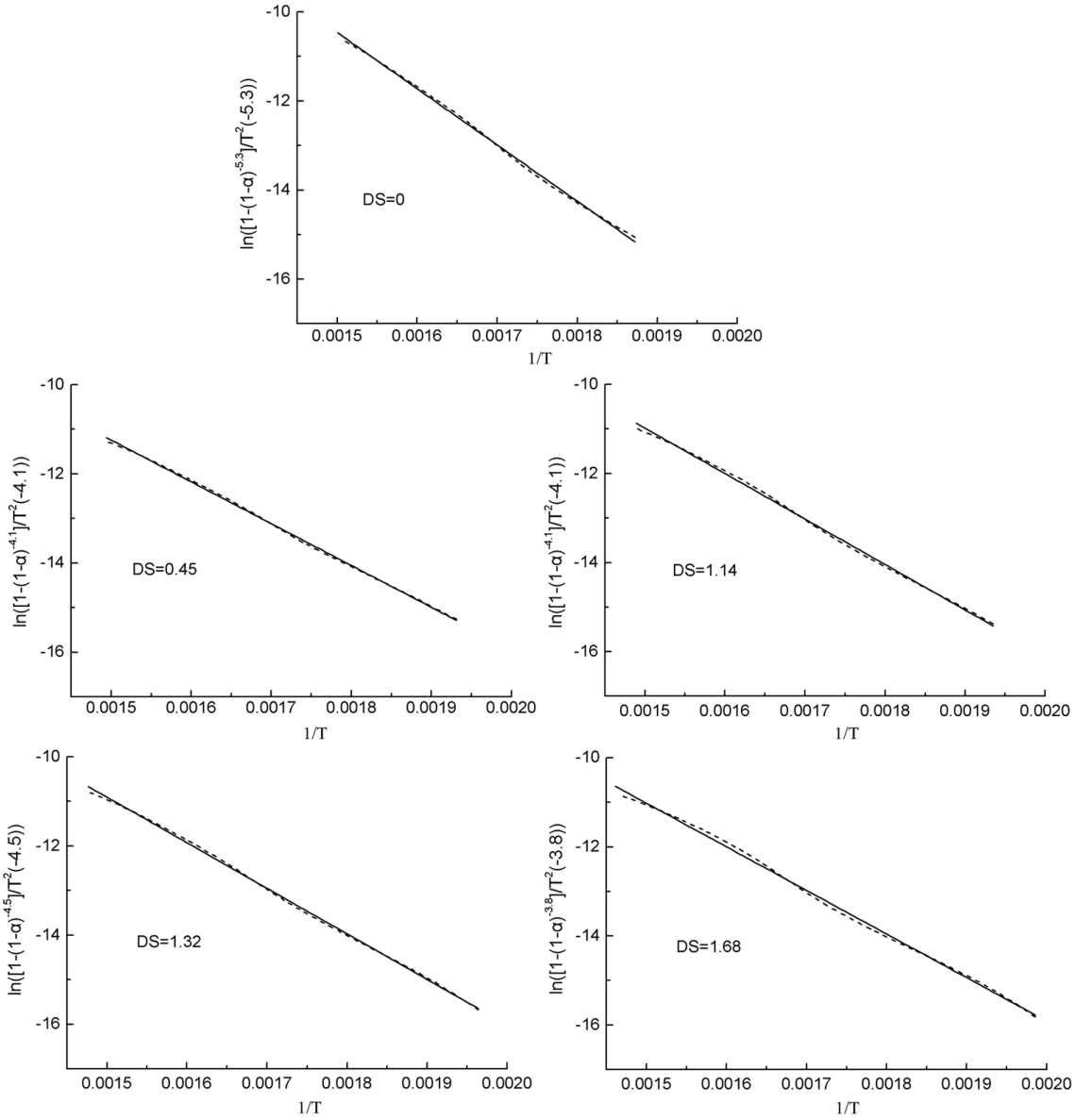

Fig. 9. Coats-Redfern plots of original LS and butyrated LS with different DS in the fast pyrolysis stage at 10 °C/min

As can be seen in Table 3, the activation energies of the butyrated LS products were within the range of 78.1 to 105.0 KJ/mol during the fast pyrolysis stage, higher than indicated by the results described in other works (8 to 68 KJ/mol) (Murugan *et al.* 2008). This may be because different species of lignin were used and because of the erroneous assumption by other researchers that the thermal degradation of lignin follows first-order reaction kinetics (Jiang *et al.* 2010).

Also, as can be seen in Table 3, butyrated LS products had lower pyrolysis activation energies than unmodified LS, indicating that their pyrolytic degradation was less temperature-sensitive and less energy was required to decompose the butyrated LS, further indicating that the thermal stability of the butyrated LS products decreased following butyrylation.

Table 3. Kinetic Parameters of Butyrated LS with Different DS

DS	Temperature (°C)	n	Fitting formula	A (min^{-1})	Activation Energy (KJ/mol)	R^2
0	261.09 to 393.29	6.4	y=-12627.13x+8.48	608290.84	104.98	0.9987
0.45	244.74 to 396.33	5.1	y=-9387.26x+2.84	1606.79	78.05	0.9992
1.14	243.77 to 398.53	5.1	y=-10206.0x+4.33	7750.61	84.85	0.9986
1.32	236.13 to 404.10	5.5	y=-10226.52x+4.44	8669.17	85.02	0.9991
1.68	230.54 to 411.48	4.8	y=-9789.14x+4.91	13278.39	81.39	0.9978

CONCLUSIONS

1. Butyration of LS with butyric anhydride in the presence of choline chloride is a promising method to produce LS esters rapidly and without the use of toxic catalysts. The DS of butyrated LS products determined using FTIR data increased from 0 to 0.41 to 2.14 with the addition of choline chloride. The maximum DS of 2.14 was obtained using 15 wt.% choline chloride at 120 °C for 10 min.
2. Fourier transform infrared and ^{1}H NMR spectroscopy both indicate the occurrence of the butyration reaction of LS and confirm that esterification reactions occurred at both phenolic and aliphatic hydroxyl groups.
3. Butyrated LS products were less thermodynamically stable than unmodified LS, and their thermal stability decreased with increasing DS.
4. The pyrolysis of butyrated LS was not first-order, and the thermal degradation activation energy of LS butyrate ranged from 78.1 to 105.0 KJ/mol in the fast pyrolysis stage, depending on the DS.
5. Since choline chloride is a cheap, commercially available, environmentally friendly reagent, this new methodology provides a cost-efficient and environmentally friendly approach for the chemical modification of lignin.

ACKNOWLEDGMENTS

This project was supported by the National Natural Science Foundation of China (31170516, 31470581) and the Fundamental Research Funds for the Central Universities (DL12EB03).

REFERENCES CITED

Alonso, M. V., Rodríguez, J. J., Oliet, M., Rodríguez, F., García, J., and Gilarranz, M. A. (2001). "Characterization and structural modification of ammonic lignosulfonate by methylolation," *J. Appl. Polym. Sci.* 82(11), 2661-2668. DOI: 10.1002/app.2119

Bahl, K., and Jana, S. C. (2014). "Surface modification of lignosulfonates for reinforcement of styrene-butadiene rubber compounds," *J. Appl. Polym. Sci.* 131(7), DOI: 10.1002/app.40123

Bridson, J. H., van de Pas, D. J., and Fernyhough, A. (2013). "Succinylation of three different lignins by reactive extrusion," *J. Appl. Polym. Sci.* 128(6), 4355-4360. DOI: 10.1002/app.38664

Cachet, N., Camy, S., Mlayah, B. B., Condoret, J. S., and Delmas, M. (2014). "Esterification of organosolv lignin under supercritical conditions," *Ind. Crop. Prod.* 58, 287-297. DOI: 10.1016/j.indcrop.2014.03.039

Canetti, M., De Chirico, A., and Audisio, G. (2004). "Morphology, crystallization and melting properties of isotactic polypropylene blended with lignin," *J. Appl. Polym. Sci.* 91(3), 1435-1442. DOI: 10.1002/app.13311

Chadlia, A., and Farouk, M. M. (2011). "Rapid homogeneous esterification of cellulose extracted from *Posidonia* induced by microwave irradiation," *J. Appl. Polym. Sci.* 119(6), 3372-3381. DOI: 10.1002/app.32973

Chang, H. T., Su, Y. C., and Chang, S. T. (2006). "Studies on photostability of butyrylated, milled wood lignin using spectroscopic analyses," *Polym. Degrad. Stabil.* 91(4), 816-822. DOI: 10.1016/j.polymdegradstab.2005.06.010

Chen, D., Zhang, A. P., Liu, C. F., and Sun, R. C. (2012). "Modification of sugarcane bagasse with acetic anhydride and butyric anhydride in ionic liquid 1-butyl-3-methylimidazolium chloride," *BioResources* 7(3), 3476-3487. DOI: 10.15376/biores.7.3.3476-3487

Faix, O. (1991). "Classification of lignins from different botanical origins by FT-IR spectroscopy," *Holzforschung* 45(s1), 21-27. DOI: 10.1515/hfsg.1991.45.s1.21

Flynn, J. H. (1989). *Thermal Analysis in Encyclopedia of Polymer Science and Engineering*, Wiley, New York, pg. 690.

Fox, S. C., and McDonald, A. G. (2010). "Chemical and thermal characterization of three industrial lignins and their corresponding lignin esters," *BioResources* 5(2), 990-1009. DOI: 10.15376/biores.5.2.990-1009

Gilarranz, M. A., Rodríguez, F., Oliet, M., García, J., and Alonso, V. (2001). "Phenolic OH group estimation by FTIP and UV spectroscopy. Application to organosolv lignins," *J. Wood Chem. Technol.* 21(4), 387-395. DOI: 10.1081/WCT-100108333

Glasser, W. G., Jain, R. K. (1993). "Lignin derivatives. I. Alkanoate," *Holzforschung* 47(3), 225-233. DOI: 10.1515/hfsg.1993.47.3.225

Gordobil, O., Egüés, I., Llano-Ponte, R., and Labidi, J. (2014). "Physicochemical properties of PLA lignin blends," *Polym. Degrad. Stabil.* 108(s1), 330-338. DOI: 10.1016/j.polymdegradstab.2014.01.002

Grunden, B. L., and Sung, C. S. P. (2004). "Cure characterization of unsaturated polyester resin by fluorescence spectroscopy," *J. Appl. Polym. Sci.* 94(6), 2446-2450. DOI: 10.1002/app.21189

Jiang, G., Nowakowski, D. J., and Bridgwater, A. V. (2010). "A systematic study of the kinetics of lignin pyrolysis," *Thermochim. Acta* 498(1-2), 61-66. DOI: 10.1016/j.tca.2009.10.003

Laurichesse, S., and Avérous, L. (2014). "Chemical modification of lignins: Towards biobased polymers," *Prog. Polym. Sci.* 39(7), 1266-1290. DOI: 10.1016/j.progpolymsci.2013.11.004

Lin, N., Fan, D. K., Chang, P. R., Yu, J. H., Cheng, X. C., and Huang, J. (2011). "Structure and properties of poly(butylene succinate) filled with lignin: A case of lignosulfonate," *J. Appl. Polym. Sci.* 121(3), 1717-1724. DOI: 10.1002/app.33754

Lin, Z., Renneckar, S., and Hindman, D. P. (2008). "Nanocomposite-based lignocellulosic fibers 1. Thermal stability of modified fibers with clay-polyelectrolyte multilayers," *Cellulose* 15(2), 333-346. DOI: 10.1007/s10570-007-9188-y

Lisperguer, J., Nunez, C., and Perez-Guerrero, P. (2013). "Structure and thermal properties of maleated lignin-recycled polystyrene composites," *J. Chil. Chem. Soc.* 58(4), 1937-1940.

Lopes, J. M., Paninho, A. B., Molho, M. F., Nunes, A. V. M., Rocha, A., Lourenco, N. M. T., and Najdanovic-Visak, V. (2013). "Biocompatible choline based ionic salts: Solubility in short-chain alcohols," *J. Chem. Thermodyn.* 67, 99-105. DOI: 10.1016/j.jct.2013.07.025

Maldhure, A. V., Chaudhari, A. R., and Ekhe, J. D. (2011). "Thermal and structural studies of polypropylene blended with esterified industrial waste lignin," *J. Therm. Anal. Calorim.* 103(2), 625-632. DOI: 10.1007/s10973-010-1048-6

Maldhure, A. V., Ekhe, J. D., and Deenadayalan, E. (2012). "Mechanical properties of polypropylene blended with esterified and alkylated lignin," *J. Appl. Polym. Sci.* 125(3), 1701-1712. DOI: 10.1002/app.35633

Murugan, P., Mahinpey, N., Johnson, K. E., and Wilson, M. (2008). "Kinetics of the pyrolysis of lignin using thermogravimetric and differential scanning calorimetry methods," *Energ. Fuel.* 22(4), 2720-2724. DOI: 10.1002/app.35633

Pu, Y., Jiang, N., and Ragauskas, A. J. (2007). "Ionic liquid as a green solvent for lignin," *J. Wood Chem. Technol.* 27(1), 23-33. DOI: 10.1080/02773810701282330

Sailaja, R. R. N., and Deepthi, M. V. (2010). "Mechanical and thermal properties of compatibilized composites of polyethylene and esterified lignin," *Mater. Design* 31(9), 4369-4379. DOI: 10.1016/j.matdes.2010.03.046

Sait, H. H., Hussain, A., Salema, A. A., and Ani, F. N. (2012). "Pyrolysis and combustion kinetics of date palm biomass using thermogravimetric analysis," *Bioresource Technol.* 118, 382-389. DOI: 10.1016/j.biortech.2012.04.081.

Singh, B., Lobo, H., and Shankarling, G. (2011). "Selective N-alkylation of aromatic primary amines catalyzed by bio-catalyst or deep eutectic solvent," *Catal. Lett.* 141(1), 178-182. DOI: 10.1007/s10562-010-0479-9

Tejado, A., Peña, C., Labidi, J., Echeverria, J. M., and Mondragon, I. (2007). "Physico-chemical characterization of lignins from different sources for use in phenol-formaldehyde resin synthesis," *Bioresource Technol.* 98(8), 1655-1663. DOI: 10.1016/j.biortech.2006.05.042

Thielemans, W., and Wool, R. P. (2004). "Butyrated kraft lignin as compatibilizing agent for natural fiber reinforced thermoset composites," *Compos. Part A-Appl. S.* 35(3), 327-338. DOI: 10.1016/j.compositesa.2003.09.011

Thielemans, W., and Wool, R. P. (2005). "Lignin esters for use in unsaturated thermosets: Lignin modification and solubility modeling," *Biomacromolecules* 6(4), 1895-1905. DOI: 10.1021/bm0500345

Tjeerdsma, B. F., and Militz, H. (2005). "Chemical changes in hydrothermal treated wood: FTIR analysis of combined hydrothermal and dry heat-treated wood," *Holz als Roh- und Werkstoff* 63(2), 102-111. DOI: 10.1007/s00107-004-0532-8

Wang, Z., Yang, X., Zhou, Y., and Liu, C. (2013). "Mechanical and thermal properties of polyurethane films from peroxy-acid wheat straw lignin," *BioResources* 8(3), 3833-3843. DOI: 10.15376/biores.8.3.3833-3843

Watanabe, A., Morita, S., Kokot, S., Matsubara, M., Fukai, K., and Ozaki, Y. (2006). "Drying process of microcrystalline cellulose studied by attenuated total reflection IR

spectroscopy with two-dimensional correlation spectroscopy and principal component analysis," *J. Mol. Struct.* 799(1-3), 102-110. DOI: 10.1016/j.molstruc.2006.03.018

Wyman, I. W., and Macartney, D. H. (2010). "Cucurbit[7]uril host-guest complexes of cholines and phosphonium cholines in aqueous solution," *Org. Biomol. Chem.* 8(1), 253-260. DOI: 10.1039/b917610a

Xiao, B., Sun, X. F., and Sun, R. C. (2001). "The chemical modification of lignins with succinic anhydride in aqueous systems," *Polym. Degrad. Stabil.* 71(2), 223-231. DOI: 10.1016/S0141-3910(00)00133-6

Yadav, U. N., and Shankarling, G. S. (2014). "Synergistic effect of ultrasound and deep eutectic solvent choline chloride-urea as versatile catalyst for rapid synthesis of β-functionalized ketonic derivatives," *J. Mol. Liq.* 195, 188-193. DOI: 10.1016/j.molliq.2014.02.016

Ye, D. Z., Zhang, M. H., Gan, L. L., Li, Q. L., and Zhang, X. (2013). "The influence of hydrogen peroxide initiator concentration on the structure of eucalyptus lignosulfonate," *Int. J. Biol. Macromol.* 60, 77-82. DOI: 10.1016/j.ijbiomac.2013.05.016

Zakzeski, J., Bruijnincx, P. C. A., Jongerius, A. L., and Weckhuysen, B. M. (2010). "The catalytic valorization of lignin for the production of renewable chemicals," *Chem. Rev.* 110(6), 3552-3599. DOI: 10.1021/cr900354u

Article submitted: December 2, 2014; Peer review completed: February 9, 2015; Revised version received and accepted: March 3, 2015; Published: April 14, 2015.
DOI: 10.15376/biores.10.2.3181-3196